$H^+ - O^+$ Coulomb Collision Frequency in the Polar Wind Plasma

تردد التصادم بين أيونات الهيدروجين والأكسجين في بلازما الرياح القطبية

**Imad Barghouthi*, Mazen Abu Issa*, Mahmoud Abu Samra*,
Naji Qatanani**[**]

*Department of Physics, [**]Department of Mathematics,

Faculty of Science, Al-Quds University, Jerusalem, Palestine.

E-mail: barghouthi@yahoo.com

Abstract

The polar wind is an ambipolar plasma outflow from the terrestrial ionosphere at high latitudes. As the ions drift upward along geomagnetic flux tubes, they move from collision-dominated to collisionless regions. A Monte Carlo simulation was used to calculate the H^+ temperature and $H^+ - O^+$ Coulomb collision frequency $\upsilon_{H^+-O^+}$ in the polar wind. The simulation properly accounted for the divergence of geomagnetic field lines, the gravitational force, the polarization electric field, and $H^+ - O^+$ Coulomb collisions. The H^+ temperature was found to increase with altitude and then decreases due to the interplay between frictional heating due to Coulomb collisions and adiabatic cooling (due to diverging geomagnetic field). The Coulomb collision frequency $\upsilon_{H^+-O^+}$ was found to decrease with altitude. As altitude increases, the H^+ ions are accelerated by the upward directed ambipolar electric field and become less coupled with the background ions. One of the objectives is to study the consequences of a velocity distribution function with an enhanced high energy tail for the injected H^+ ions. As the number of high energy H^+ ions increases in the tail of the H^+ velocity distribution at the injection point (i.e. kappa parameter decreases), the H^+ temperature increases and $\upsilon_{H^+-O^+}$ decreases.

Key words: Polar wind, Coulomb collision frequency, Kappa distribution, Monte Carlo simulation.

ملخص

إن بلازما الرياح القطبية تكون مؤلفة أساسا من أيونات الأكسجين والهيدروجين بالإضافة إلى الإلكترونات، حيث تتمكن هذه الأيونات من التغلب على قوة الجاذبية الأرضية لها وتتمكن من الإفلات إلى

ارتفاعات أعلى. وهذه الحركة بسبب التسارع الذي تكتسبه بواسطة المجال الكهربائي المتواجد في المنطقة القطبية. استهدفت هذه الدراسة حساب تردد التصادم بين أيونات الهيدروجين وأيونات الأكسجين في الرياح القطبية باستخدام تقنية مونت كارلو حيث تمت محاكاة حركة أيون الهيدروجين في وسط تتوزع فيه أيونات الأكسجين تبعا لقانون توزيع السرعة لماكسويل. وتوصلت الدراسة إلى أن تردد التصادم يعتمد على الكثافة العددية لأيونات الأكسجين المتواجدة في الرياح القطبية ودرجة حرارة كل من أيونات الهيدروجين وأيونات الأكسجين حيث وجد أن تردد التصادم يتناقص مع الارتفاع.

1. Introduction

The polar wind is an ambipolar flow of plasma out of the high latitude ionosphere along 'open' geomagnetic field lines originating from the polar caps. Figure 1- shows a schematic representation of the different collisions regimes of H$^+$ outflow in the polar wind. There are two main regions: 1. The collision - dominated region where the ions behave like a fluid. A large number of hydrodynamic models were developed to study the behavior of the polar wind plasma in that region [1-3]. 2. The collisionless region where the individual-ion characteristics dominate the ion motion. Different models were used to study the behavior of H$^+$ in the that region, hydromagnetic [4], kinetic [5-7] and semi kinetic [8-9]. The above two regions are separated by a narrow transition layer [10-12]. where the H$^+$ behavior changes rapidly from collision-dominated to collisionless. Generalized transport models [13] are promising in the collision-dominated and collisionless regions, while their validity in the transition region has not yet been established. Barghouthi et al. [10-11] used an improved collision model (Fokker-Planck expression for H$^+$ − O$^+$ Coulomb collisions) to model the H$^+$ polar wind. They found that the adopted collision model can have a large effect on the moments of the H$^+$ velocity distribution function. Recently, Barghouthi et al. [14] used a Monte Carlo simulation to study the effect of kappa H$^+$ distributions in the polar wind. The only difference with the Monte Carlo simulation presented in Barghouthi et al.[11] concerns the distribution function f_{H^+} at the low altitude boundary, the H$^+$ velocity distribution is assumed to be a kappa distribution instead of a Maxwellian distribution.
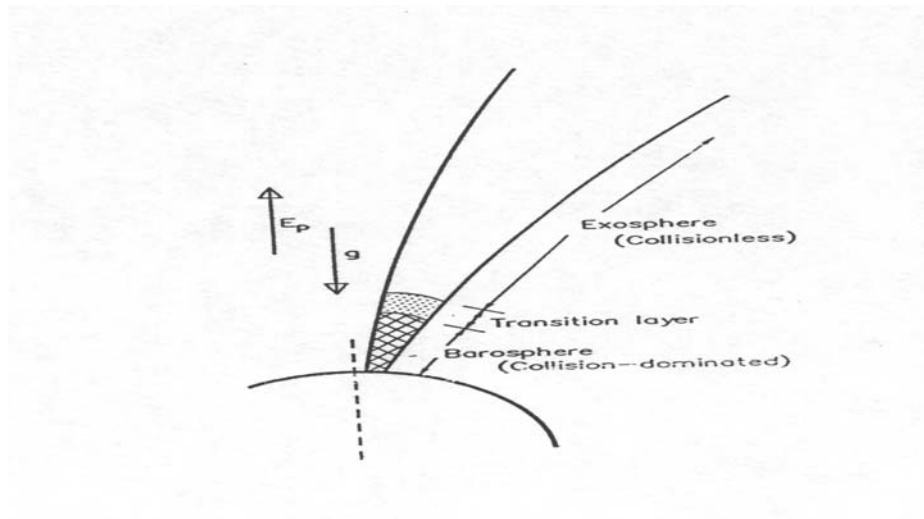
Figure 1. A schematic diagram for the flow of the polar wind plasma along diverging geomagnetic field lines. The different regimes of the ion outflow are shown, namely, the barosphere where collision-dominated conditions prevail, the exosphere where collisionless conditions prevail, and the transition region embedded in between [11].

In this paper we focus on the altitude profiles of $H^+ - O^+$ collision frequencies in the polar wind. We will use the Monte Carlo results of Barghouthi et al. [11] to calculate the $H^+ - O^+$ Coulomb collision frequency in the polar wind.

2. Theoretical Formulation

In this study we will follow the motion of H^+ from the collision-dominated region, through the transition layer, and into the collisionless region as shown in Figure 1. The minor H^+ ions are treated as test particles diffusing across a background of O^+ ions and electrons. Coulomb collisions between H^+ and O^+ are represented by a Fokker-Planck collision operator. The H^+ velocity distribution function f_{H^+} is governed by the Boltzmann equation[15]

$$\frac{\partial f_{H^+}}{\partial t} + \mathbf{V}_{H^+} \bullet \nabla f_{H^+} + \left[\mathbf{G} + \frac{e_{H^+}}{m_{H^+}} \left(\mathbf{E} + \frac{1}{c} \mathbf{V}_{H^+} \times \mathbf{B} \right) \right] \bullet \nabla V_{H^+} \, f_{H^+} =$$

$$\int d\mathbf{V}_{O^+} \, d\Omega \, g \, \sigma(g, \chi) \left[f'_{H^+} f'_{O^+} - f_{H^+} f_{O^+} \right] \qquad (1)$$

where **v** is the velocity, *G* is the gravitational acceleration, *e* and *m* are the charge and mass, respectively. **E** and **B** are the electric and geomagnetic fields, *c* is the speed of light, $\mathbf{g} \equiv \mathbf{V}_{H^+} - \mathbf{V}_{O^+}$ is the relative velocity, $d\Omega$ is the element of solid angle, σ is the differential scattering cross section, and χ is the scattering angle. The primes denote quantities evaluated after collision. The O$^+$ ions are assumed to be in static equilibrium and, consequently, their distribution function f_{O^+} is assumed to have local Maxwellian that depends on the altitude *z*.

$$f_{O^+} = n_{O^+}(z) \left(\frac{m_{O^+}}{2\pi k T_{O^+}} \right)^{3/2} \exp\left(-\frac{m_{O^+} v_{O^+}^2}{2 k T_{O^+}} \right) \qquad (2)$$

where n_{o+} is the number density, *k* is the Boltzmann constant, and *T* is the temperature.

The right hand side of equation (1) (i.e. the collision term) reduces to the well known Fokker-Planck form for H$^+$ – O$^+$ Coulomb collisions as given by Barghouthi et al. [11].

Collision term

$$= -\frac{\partial}{\partial v_{H^+}} \bullet \left[A_{H^+} f_{H^+} - \frac{1}{2}\frac{\partial}{\partial v_{H^+}} \bullet \left(\mathbf{D}_{H^+} f_{H^+} \right) \right] \tag{3}$$

where A_{H^+} is the friction coefficient and D_{H^+} is the diffusion coefficient tensor given by

$$\mathbf{D}_{H^+} = D_{H^+ 11}\, \mathbf{e}_z \mathbf{e}_z + D_{H^+ \perp}\left(\mathbf{I} - \mathbf{e}_z \mathbf{e}_z \right) \tag{4}$$

the expressions for $\mathbf{A}_{H^+}$, $D_{H^+ 11}$ and $D_{H^+ \perp}$ are given by Hinton [16] and are not repeated here.

3. Monte Carlo Simulation

We consider the steady state flow of a plasma that is composed of H^+, O^+ and electrons. The H^+ ions are treated as test particles, which implies that H^+ is minor such that $H^+ - H^+$ collisions are neglected in comparison with $H^+ - O^+$ collisions, and that the electron density is approximately equal to the O^+ density. The effects of gravity, polarization electric field, and diverging geomagnetic field are included. For simplicity the electron and O^+ temperatures are assumed to be constant. The electrons are assumed to obey the Boltzmann relation. Since O^+ ions are bound due to gravity, they were assumed to be in diffusive-equilibrium and to have a corresponding local non-drifting Maxwellian velocity distribution at all altitudes, as given in equation 2.

Barghouthi et al. [11] assumed that H^+ velocity distribution f_{H^+} at the lower boundary in the collision-dominated region to be close to a Maxwellian

$$f_{H^+} = n_{H^+}(z_o) \left(\frac{m_{H^+}}{2\pi k T_{H^+}} \right)^{3/2} \exp\left(-\frac{m_{H^+} v_{H^+}^2}{2 k T_{H^+}} \right) \tag{5}$$

where $n_{H^+}(z_o)$ is the number density at the boundary level z_o.

Recently, Barghouthi et al. [14] assumed the H^+ velocity distribution to be a kappa function at the lower boundary in the collision-dominated region.

$$f_{H^+} = \frac{n_{H^+}(z_o)\Gamma(\kappa+1)}{(\pi\kappa w^2)^{3/2}\,\Gamma\left(\kappa-\frac{1}{2}\right)}\left(1+\frac{v^2}{\kappa w^2}\right)^{-(k+1)} \tag{6}$$

where $\Gamma(x)$ is the Gamma function, $w=\sqrt{(2\kappa-3)kT/\kappa m_{H^+}}$ is the thermal speed, κ is a spectral index which has to be greater than $\frac{3}{2}$, unless the f_{H^+} function has unphysical moments. Different examples of kappa functions are shown in Figure 2 [17].
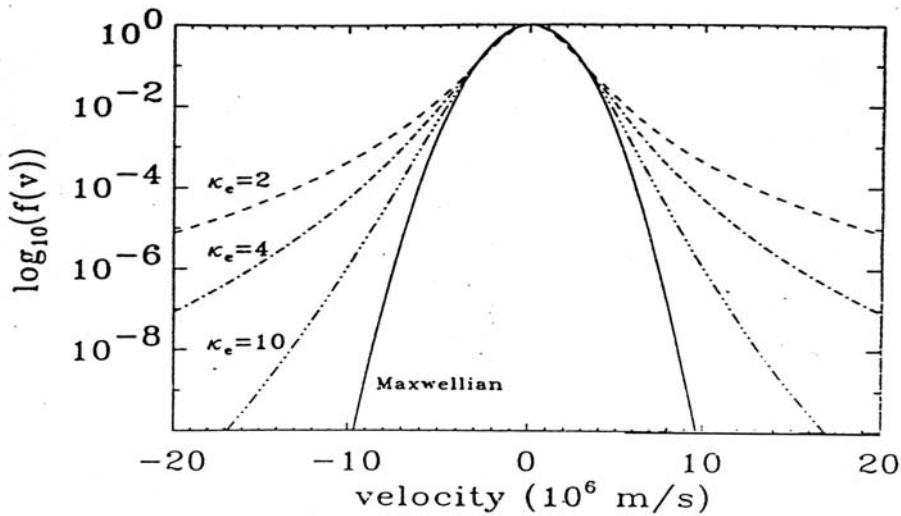

Figure (2) Different examples of kappa velocity distribution functions, all normalized to the same value at $v=0: f(0)=1$. One can see that in the limit $\kappa \to +\infty$, the function approaches to a Maxwellian or Gaussian function (solid line) [17].

In this study we will use the obtained results of Barghouthi et al. [11, 14] to produce an altitude profile for T_{H^+} and to use this temperature to calculate the $H^+ - O^+$ Coulomb collision frequency at different altitudes. For $H^+ - O^+$ Coulomb collision frequency we adopted the following form

$$\nu_{H^+-O^+} = \frac{1.23 n_{O^+}(z)}{\left(T_{H^+-O^+}\right)^{3/2}}$$

(7)

where $T_{H^+-O^+} = \dfrac{m_{O^+} T_{H^+} + m_{H^+} T_{O^+}}{m_{H^+} + m_{O^+}}$

More details about $\upsilon_{H^+-O^+}$ are given in Schunk [15].

4. Results

A total number of 10^5 H^+ test ions are injected (one at a time) into the simulation region at the lower boundary (500 km) with an initial random velocity. The H^+ ion moves under the influence of the external forces indicated above and is scattered by elastic Coulomb collisions, until it leaves the simulation region at the topside (6000 km) or lower boundary (500 km). The density of O^+ ions at the lower boundary is $n\left(O^+\right) = 10^6 \, cm^{-3}$.

The temperatures of electrons and O^+ ions are assumed to be equal to 2500 K in the simulation region.

Barghouthi et al. [14] assumed the H^+ distribution function to be a kappa function at lower boundary of the simulation tube. For H^+ ions of lowest velocities, the kappa function is very similar to the Maxwellian with the same thermal speed. However, at higher velocities the kappa function decreases as a power law of v^2 instead of exponentially. The smaller the parameter κ (Figure 2), the more enhanced the tail of the distribution with suprathermal H^+ ions. As the index κ increases the kappa function approaches the Maxwellian distribution [18].

Figure 3 shows the profiles of the H^+ temperatures. Deep in the barosphere (i.e. at low altitudes) H^+ temperature is closer to the background O^+ temperature due to strong collision coupling between H^+ and O^+. As altitude increases, the H^+ drift velocity increases [14] and hence T_{H^+} increases due to frictional heating with the background O^+ ions. At 2000 km, T_{H^+} reaches a maximum and then decreases due to parallel and perpendicular

adiabatic cooling [11, 19-20]. As the spectral index κ of kappa function decreases $(100 \rightarrow 2)$ the distribution function $f_{\mathrm{H^+}}$ at the lower boundary goes from Maxwellian to kappa function.
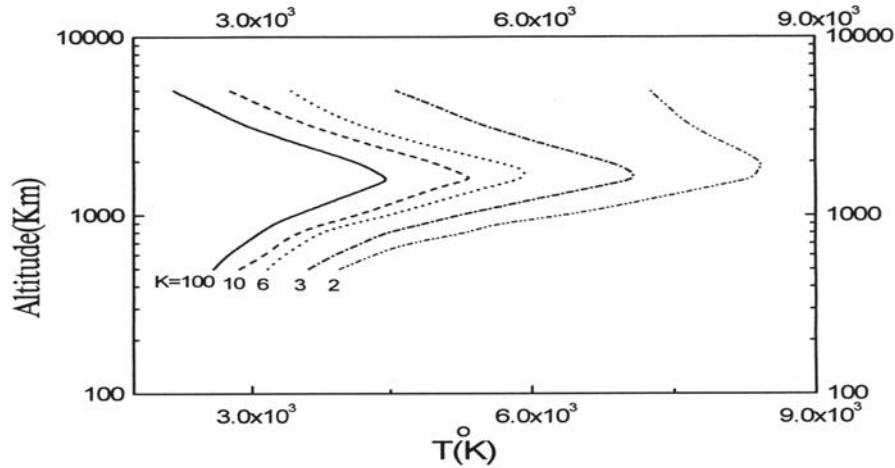

Figure 3. Altitude profiles of $\mathrm{H^+}$ temperatures obtained with Monte Carlo simulations for different values of κ at the lower boundary altitude: κ =100 or Maxwellian (solid line) κ =10 (dashed line), κ =6 (dotted line), κ =3 (dashed-dotted line), and κ =2 (two dots-dashed line). At the lower boundary altitude (500 km), $T_{O^+} = 2500°\mathrm{K}$ and $n_{O^+} = 10^6\, cm^{-3}$.

According to figure 2, the number of $\mathrm{H^+}$ ions in the tail of kappa function increases (i.e. the number of $\mathrm{H^+}$ ions with high velocities increases) this explains the increase in $T_{\mathrm{H^+}}$ as κ decreases.

The most interesting result in this study is the altitude profile for $\upsilon_{\mathrm{H^+ - O^+}}$ Coulomb collisions frequency displayed in figure 4. As shown in figure 4, at low altitudes and for large values of κ, the majority of particles are in the bulk not in the tail of the distribution. As we know, the relative velocity between $\mathrm{H^+}$

and O^+ ions is $\mathbf{g} \left[\equiv \mathbf{V}\left(H^+ \right) - \mathbf{V}\left(O^+ \right) \right]$ and the Coulomb scattering cross

section is proportional to g^{-3}. Due to this fact the H^+ ions in the bulk of the distribution are strongly coupled with the O^+ background ions and those in the tail are less coupled. As the ions move upward their velocity become very large[14], and less coupled with the background particles. Due to these considerations we can explain the profile of $\upsilon_{H^+-O^+}$. For large values of κ, $\kappa = 100$ (i.e. Maxwellian case) the number of $H^+ - O^+$ collisions is very high, nine collisions per second. As the altitude increases, the drift velocities of H^+ ions increase, relative velocity g increases, the H^+ ions become less coupled with the O^+ of the background, consequently $\upsilon_{H^+-O^+}$ decreases. The behavior of $\upsilon_{H^+-O^+}$ shows that the number of collisions decreases from nine at 500 km to one at 1000 km and approximates zero (collisionless) at higher altitudes.
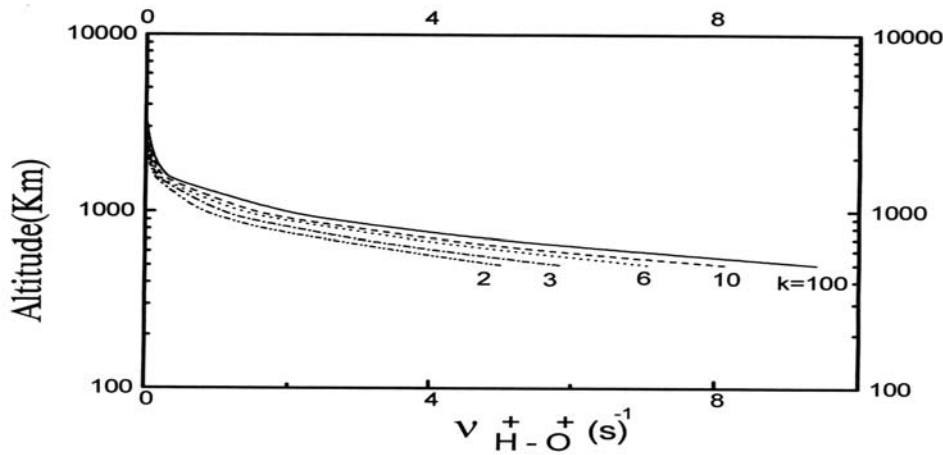

Figure 4. Altitude profiles of $H^+ - O^+$ coulomb collision frequencies obtained with Monte Carlo simulations for different values of κ at the lower boundary altitude: $\kappa = 100$ or Maxwellian (solid line), $\kappa = 10$ (dashed line), $\kappa = 6$ (dotted line), $\kappa = 3$ (dashed-dotted line), and $\kappa = 2$ (two dots-dashed line). At the lower boundary altitude (500 km), $T_{O^+} = 2500°K$ and $n_{O^+} = 10^6 \, cm^{-3}$.

As the spectral index κ decreases, the number of H^+ ions increases in the tail of f_{H^+}, (i.e. there are many of H^+ ions with high velocities). As a result the number of $H^+ - O^+$ collisions decreases when κ decreases, (e.g. at 500 km for κ=100, $\upsilon_{H^+ - O^+} = 9 s^{-1}$, while for κ=2, $\upsilon_{H^+ - O^+} = 5 s^{-1}$). At high altitudes the effect of κ index is negligible because all H^+ ions have large velocities and they are not coupled with O^+ ions (i.e. collisionless).

5. Conclusion

We have used a Monte Carlo simulation to calculate the $H^+ - O^+$ Coulomb collision frequency in the polar wind plasma. The simulation region included the collision-dominated region (low altitudes), the collisionless region (high altitudes and the transition region (intermediate altitudes). The effects of gravitational force, polarization electric field, divergence geomagnetic field, and $H^+ - O^+$ Coulomb collisions were taken into consideration. We used the Fokker-Planck form for $H^+ - O^+$ particle interactions. The velocity distribution of H^+ ions injected at the bottom (500 km) of the simulation region is assumed to be a generalized Lorentzian function with a parameter kappa κ (i.e. kappa distribution). Our main findings may be summarized as follows:

1. The H^+ temperature attain its maximum at altitude 1500 km as a result of the competition between frictional heating (which dominates at low altitude due to Coulomb collisions with the background particles) and adiabatic cooling [20] (which dominates at high altitudes due to diverging geomagnetic field).
2. As kappa parameter decreases, H^+ temperature increases due to the increasing number of H^+ ions in the tail of the velocity distribution.
3. $H^+ - O^+$ collision frequency $\upsilon_{H^+ - O^+}$ decreases with altitude. As altitude increases, the velocities of H^+ ions increases [14], consequently, H^+ ions become less coupled with the background, since Coulomb collision cross section is proportional to g^{-3}, where g is the relative velocity $\left(\upsilon_{H^+} - \upsilon_{O^+}\right)$.
4. As kappa parameter decreases, the number of H^+ ions in the tail of the distribution increases. Those ions in the tail of the velocity distribution have large velocities, therefore, they are less coupled with the ions of the background, consequently, the number of H^+ collisions with O^+ ions decreases.

References

1) Banks, P.M., & Holzer, T.E., "The polar wind", *J. Geophysics Res.,* **73**, (1968), 6846-6854,.

2) Raitt, W.J., Schunk, R.W., & Banks, P.M., "A comparison of the temperature and density structure in high and low speed thermal proton flows", *Planet. Space Sci.*, **23**, (1975), 1103-1117.

3) Gombosi, T.I., & Rasmussen, C.E., "The transport of gyration-dominated space plasmas of thermal origin, I Generalized transport equations", *J. Geophysics Res.*, **96**, (1991), 7759-7778.

4) Holzer, T.E., Fedder, J.A., & Banks, P.M., "A comparison of kinetic and hydrodynamic models of an expanding ion-exosphere", *J. Geophysics Res.*, **76**, (1971), 2453-2468.

5) Lemaire, J., "O^+, H^+, and He^+ ion distribution in a new polar wind model", *J. Atmos. Terr.Phys.*, **34**, (1972), 1647-1658,.

6) Lemaire, J., & Scherer, M., "Kinetic models of the solar and polar winds", *Rev. Geophysics*, **11**, (1973), 427-468.

7) Lemaire, J., & Scherer, M., "Model of the polar ion-exosphere", *Planet. Space Sci.*, **18**, (1970), 103-120.

8) Barakat, A.R., & Schunk, R.W., "O^+ ions in the polar wind", *J. Geophysics Res.*, **88**, (1983), 7887-7894.

9) Barakat, A.R., & Schunk, R.W., "Effect of hot electrons on the polar wind", *J. Geophysics Res.*, **89**, 9771-9783, 1984.

10) Barghouthi, I.A., Barakat, A.R., Schunk, R.W., & J., "Lemaire, H^+ outflow in the polar wind: A Monte Carlo simulation", *EoS Trans. AGU.*, **71**, (1990), 1493.

11) Barghouthi, I.A., Barakat, A.R., & Schunk, R.W., "Monte Carlo study of the transition region in the polar wind: An improved collision model", *J. Geophysics Res.*, **98**, (1993), 17.583-17.591.

12) Barakat, A.R., Barghouthi, I.A., & Schunk, R.W., "Double-Hump H^+ velocity distribution in the polar wind", *Geophysics Res. Lett.*, **22**, (1995), 1857-1860.

13) Demars, H.G., & Schunk, R.W., "Comparison of solutions to bi-Maxwellian and Maxwellian transport equations for subsonic flows", *J. Geophysics Res.*, **92**, (1987), 5969.

14) Barghouthi, I.A., Pierrard, V., Barakat, A.R., & Lemaire, J., "A Monte Carlo simulation of the H^+ polar wind: Effect of velocity distributions with kappa suprathernal tails", *Astrophysics and Space Science*, **277**, (2001), 427-436.

15) Schunk, R.W., "Mathematical structure of transport equations for multispecies flows", *Rev. Geophysics*, **15**, (1977), 429-445.

16) Hinton, F.L., "Collisional transport in plasma, in Basic plasma physics I", edited by A.A. Galeev and R.N. Sudan, North-Holland, New York, (1983), 147-197.

17) Maksimovic, M., Pierrard, V., & Lemaire, J. F., "A kinetic model of the solar wind with kappa distibution functions in the corona", *Astronomy and Astrophysics*, **324**, (1997), 725-734.

18) Pierrard, V., & Lemaire, J.F., "Lorentzian ion exosphere model", *J. Geophysics Res.*, **101**, (1996), 7923.

19) Barghouthi, I.A., Barakat, A.R., & Persoon, A.M., "Effects of altitude-dependent wave-particle inteactions on the polar wind plasma", *Astrophysics and Space Science*, **259**, (1998), 117-140.

20) Barghouthi, I.A., "Effects of wave-particle interactions on $\mathbf{H}^+$ and $\mathbf{O}^+$ outflow at high latitudes: A comparative study", *J. Geophysics. Res.*, **102**, (1997), 22.065-22.075.